Thallium-201 in Brain Tumors: Relationship between Tumor Cell Activity in Astrocytic Tumor and Proliferating Cell Nuclear Antigen

Masatoshi Ishibashi, Akira Taguchi, Yasuo Sugita, Seiichiro Morita, Seiji Kawamura, Noriyoshi Umezaki, Minoru Shigemori and Naofumi Hayabuchi

Divisions of Nuclear Medicine and Nuclear Medical Technology, Department of Radiology and Department of Neurosurgery, Radioisotope Institute for Basic and Clinical Medicine, Kurume University School of Medicine, Fukuoka, Japan

This study was performed to assess the relationship between ^{201}Tl chloride uptake and brain tumor proliferation using monoclonal antibody Ki-67 and proliferating cell nuclear antigen (PCNA). **Methods:** Thirty-four patients with brain tumors were studied. Serial SPECT images were recorded and thallium uptake (Tl index) and washout rates in the tumors were calculated. Imaging results were compared with those from biopsy and histology. Cell proliferation was determined by PCNA or Ki-67 monoclonal antibody staining. **Results:** Thallium-201-chloride indices of the astrocytoma were 1.73 ± 0.17 and 1.48 ± 0.07 on early and delayed images, respectively. On the other hand, ^{201}Tl indices for anaplastic astrocytoma were 2.60 ± 1.05 and 1.76 ± 0.93 and 3.26 ± 1.63 and 2.23 ± 0.56 for glioblastoma. The correlation coefficient between ^{201}Tl and PCNA indices was 0.68 for astrocytic tumors. There was no statistically significant correlation between the ^{201}Tl (delay) and Ki-67 indices for astrocytic tumor. There were no significant differences between Ki-67/PCNA indices and washout rates. **Conclusion:** There was a positive correlation between PCNA but not the Ki-67 labeling index and the ^{201}Tl index. With the use of a noninvasive technique, ^{201}Tl index supports the PCNA index.

Key Words: thallium-201; astrocytoma; anaplastic astrocytoma; glioblastoma

J Nucl Med 1995; 36:2201–2206

Ideal radiopharmaceuticals for tumor localization have high affinity for neoplastic tissues. PET has played an important role in identifying recurrent glioblastoma utilizing metabolic tracers such as ^{18}F-fluorodeoxyglucose ([^{18}F]FDG) and ^{11}C-putresine (*1*). Increased glucose and amino acid uptake in glial tumors measured by PET with [^{18}F]FDG and ^{11}C-putresine have been reported to accurately identify the malignancy grade of lesions and predict the clinical outcome. Although these methods appear promising, the limited availability of PET instruments restricts this diagnostic modality to only a few centers around the world.

Thallium-201 has been used for myocardial imaging and facilitates evaluation of myocardial viability. In the course of performing myocardial imaging, Tonami and Hisada (*2*) incidentally found increased uptake of ^{201}Tl in lung carcinoma. Subsequently, ^{201}Tl has been used for various tumors, including esophageal cancer and primary (*3–5*) and metastatic (*6*) brain tumors. Ancri et al. (*4,6*) studied patients with primary and metastatic brain tumors in 1978 and 1980. These studies were extended by Kaplan et al. (*7*) in 1987, who compared the scan findings with the histopathologic results. Kim et al. (*8*) described the usefulness of the ^{201}Tl index in low-grade versus high-grade astrocytoma. These investigators compared ^{201}Tl localization in the tumor to a mirror image ROI in the contralateral hemisphere.[1]

These investigators report the comparison of ^{201}Tl uptake to histologic grade, but the relationship of histologic grade to cell proliferation has been previously reported (*9–11*). The present study uses two histologic techniques (*12,13*), identification of the proliferating cell nuclear antigen (PCNA) and the monoclonal antibody Ki-67, to define the degree of cell proliferation for comparison with ^{201}Tl imaging results.

METHODS

Patients

The study population consisted of 34 patients with brain tumors (19 men, 15 women, aged 10 to 75 yr, mean 45 yr). Histological diagnosis in all patients are summarized in Table 1. All patients were examined with contrast-enhanced CT, MRI and histologic confirmation of the lesion by biopsy or surgery. Informed consent was obtained in all cases from patients or guardians.

Tumor Classification

The histological findings are summarized in Table 1. Astrocytic tumors were divided into three groups: astrocytoma, anaplastic astrocytoma and glioblastoma. Benign tumors were divided into hypervascular and normovascular or hypovascular tumors based upon gadolinium enhancement using MRI. Hypervascular tumor comprised of meningioma, pituitary adenoma and hemangioblastoma. Normovascular or hypovascular tumors comprised of acoustic neurinoma, germinoma, craniopharingioma and central neurocytoma.

Received Sept. 1, 1994; revision accepted Mar. 13, 1995.

For correspondence or reprints contact: Masatoshi Ishibashi, MD, Division of Nuclear Medicine, Department of Radiology, Kurume University School of Medicine, 67 Asahi-Machi, Kurume-City, Fukuoka, 830, Japan.

TABLE 1
Clinical Features, Visual Analysis, Thallium-201 Findings and Ki-67 and PCNA Indices

Patient no.	Age (yr)	Sex	Diagnosis	Visual analysis		Tl index		Washout rate (%)	Ki-67 index (%)	PCNA index (%)
				E	D	E	D			
1	62	F	Astrocytoma	1	1	1.71	1.53	10.5	(−)	6.5
2	32	F	Astrocytoma	1	1	1.91	1.40	26.7	(−)	1.21
3	44	F	Astrocytoma	1	1	1.57	1.50	4.5	(−)	4.26
4	34	M	Anaplastic astrocytoma	3	3	1.81	0.90	50.3	(−)	4.12
5	31	M	Anaplastic astrocytoma	1	1	2.33	2.20	5.8	19.2	(−)
6	10	M	Anaplastic astrocytoma	1	1	2.88	0.88	53.2	6.96	2.58
7	37	M	Anaplastic astrocytoma	3	3	4.28	3.09	27.8	(−)	16.3
8	43	F	Anaplastic astrocytoma	3	3	1.72	1.71	6.40	(−)	8.06
9	46	M	Glioblastoma	3	3	2.41	1.91	20.7	8.83	12.4
10	62	M	Glioblastoma	3	3	2.28	1.78	21.9	(−)	(−)
11	37	M	Glioblastoma	1	1	1.84	1.82	1.10	15.1	1.97
12	56	M	Glioblastoma	3	3	3.10	1.86	29.7	8.99	(−)
13	40	M	Glioblastoma	3	3	2.17	1.86	14.3	(−)	(−)
14	62	M	Glioblastoma	3	3	3.07	2.52	21.2	(−)	5.82
15	75	F	Glioblastoma	3	3	6.40	3.50	45.3	15.2	14.6
16	52	M	Glioblastoma	3	3	2.25	1.84	18.2	(−)	(−)
17	63	M	Glioblastoma	3	3	6.10	2.50	59.0	16.8	46.1
18	53	F	Glioblastoma	3	3	2.95	2.68	9.15	14.6	31.2
19	38	M	Meningioma	3	—	4.82	(−)	(−)		
20	47	M	Meningioma	3	3	4.35	3.04	30.1		
21	56	M	Meningioma	3	3	4.42	2.28	48.4		
22	65	F	Meningioma	3	3	4.76	3.96	16.8		
23	41	F	Meningioma	3	1	3.57	1.35	62.1		
24	57	F	Acoustic neurinoma	3	3	2.80	2.21	21.1		
25	43	M	Acoustic neurinoma	1	1	1.92	1.00	47.9		
26	60	F	Acoustic neurinoma	1	0	(−)	(−)	(−)		
27	71	F	Pituitary adenoma	3	2	2.53	2.26	10.6		
28	54	F	Pituitary adenoma	3	3	2.82	2.30	18.4		
29	54	F	Pituitary adenoma	3	3	5.07	2.39	16.6		
30	12	F	Germinoma	3	3	4.00	2.90	27.5		
31	13	M	Germinoma	3	2	3.33	2.00	39.9		
32	21	M	Craniopharyngioma	3	2	1.30	1.14	12.3		
33	55	F	Hemagioblastoma	3	1	4.38	1.85	57.7		
34	39	M	Central neurocytoma	3	3	2.27	2.00	11.8		

E = early; D = delayed.

SPECT

SPECT was performed approximately 20 min and 4 hr after intravenous administration of ^{201}Tl (111 MBq) using a multidetector scanner equipped with a low-energy, "turbo-fan collimator." The head unit consists of two rings of 64 probe-type detectors, 9.2 cm long by 24.4 cm in diameter. Inside the ring of crystals there is a rotating collimator with septa varying from 0° to 35.2°. Both the detector ring and the collimator rotate. The sensitivity of the 64 detectors is not uniform. Based on attenuation correction using the phantom, the sensitivity of the detectors was corrected. Data were acquired for 10 min at 2 sec/view for a total of 64 views over 360°. Images were collected in a 64 × 64 matrix on a dedicated nuclear medicine computer. A 20% window centered at the 74 keV photopeak for ^{201}Tl was used.

Continuous transaxial tomograms of the brain were reconstructed after filtered backprojection with a Butterworth (cutoff frequency 0.25 cycles/pixel, order 8) and Ramachandran filter to reduce statistical noise. Thallium-201 images were corrected for tissue attenuation using a standard commercial correction routine which assumes uniform attenuation with the circular shape of the head.

Visual and Quantitative Analyses

Visual Analysis. Visual analysis, by consensus of three observers blinded to the clinical information, was performed to assess the presence or absence of ^{201}Tl uptake in brain tumors. A four-point scale was applied: 0, normal; +1, possible uptake; +2, definite, but not intense uptake; +3, very intense uptake.

Quantitative Analysis. The ^{201}Tl SPECT images were analyzed using CT and MR images for anatomical guidance. Regions of interest (ROIs) were placed manually over the selected area showing the greatest activity in the tumor. The contralateral ROIs were placed as a mirror image of the lesion ROIs.

The ^{201}Tl index was defined as the ratio of average counts per pixel in the tumor to those in the contralateral region. The washout rate of ^{201}Tl was calculated for brain tumor activity according to the following equation:

$$\text{washout rate (\%)} = (\text{initial counts} - \text{delayed counts}) \times 100/\text{initial counts}.$$

The method assumed linear clearance and was based on an extrapolation of delayed activity at 4 hr.

PCNA Immunohistochemical Assay

Paraffin-embedded tissue sections 4-mm thick fixed with 6% formalin were mounted on gelatin-coated slides and dried overnight at 37°. Sections were de-waxed and taken through graded alcohol to phosphate-buffered saline (PBS; 0.01 *M*, pH 7.4, 0.05% Triton) prior to immunostaining by the alkaline phosphatase anti-alkaline phosphatase (APAAP) method. The primary antibody comprised the Dako-PCNA monoclonal antibody at a dilution of 1:20 for 12 hr, which was found to be optimal in this assay system. Identical PCNA scores for consecutive sections of this astrocytic tumor were obtained in approximately 10 sequential assays. Five to ten randomly selected fields were photographed (power 200) and 500 to 1000 cells were examined.

Ki-67 Immunohistochemical Assay

Astrocytic tumor sections mounted on paraffined-coated slides were air-dried overnight. The Ki-67 antibody at a 1:20 dilution in 0.05 *M* Tris-HCl prepared in 0.01 *M* phosphate-buffered saline, pH 7.6, was added to the section. The specimens were stained according to the APAAP method. The preparations were then examined under a light microscope. Five to ten randomly selected fields were photographed (power 200) and 500 to 1000 cells were evaluated.

The labeling indices of Ki-67 (*14*) and PCNA were calculated by the following equation and used for detecting tumor proliferation:

$$\text{Labeling index (\%)} = (\text{number of positive-stained cells})/(\text{total number of cells}) \times 100.$$

Statistical Analysis

All quantitative data are presented as mean ± 1 s.d. Quantitative data comparison was performed by an unpaired t-test. A p value < 0.05 was considered statistically significant.

RESULTS

Histological diagnosis in patients with brain tumors and ^{201}Tl SPECT imaging results are summarized in Table 1. Thallium-201 indices for early and delayed images in patients with astrocytic tumors are summarized in Table 2. There was a significant difference ($p < 0.05$) between the ^{201}Tl index (early and delayed) for astrocytomas and glioblastomas (Fig. 1). Alternatively, there was a positive correlation ($p < 0.01$) between the ^{201}Tl index (early or delayed) on astrocytic tumors and the PCNA index (Fig. 2). There was no correlation (p = ns) between the ^{201}Tl (early) and Ki-67 indices for astrocytoma, anaplastic astrocytoma and glioblastoma (Fig. 3). There was a positive correlation between the ^{201}Tl (delayed) and Ki-67 indices for astrocytoma, anaplastic astrocytoma and glioblastoma (Fig. 3). There was no significant difference between the Ki-67 or PCNA indices and washout rates. Figure 4 shows ^{201}Tl studies for patients with astrocytoma (left), anaplastic astrocytoma (middle) and glioblastoma (right).

Benign Brain Tumors

The ^{201}Tl index on early and delayed images in patients with hypervascular and normovascular or hypovascular benign tumors are summarized in Table 2. The ^{201}Tl index of the hypervascular tumor was significantly higher ($p < 0.05$) on the early scan than that of the normovascular or hypovascular tumor (Fig. 5), but there was no significant difference between the ^{201}Tl index of the normovascular or hypovascular tumor and the hypervascular tumor on the delayed scan (Fig. 6). Furthermore, the washout rate was not significantly different between the two groups.

TABLE 2
Thallium-201 Index on Early and Delayed Images

	^{201}Tl index	
	Early image	Delayed image
Astrocytoma	1.73 ± 0.17*	1.48 ± 0.07†
Anaplastic astrocytoma	2.60 ± 1.05	1.76 ± 0.93
Glioblastoma	3.26 ± 1.63*	2.23 ± 0.56†
Hypervascular tumor	4.08 ± 0.09‡	2.48 ± 0.75
Normo or hypovascular tumor	2.60 ± 0.98‡	1.88 ± 0.71

Thallium-201 index is demonstrated as mean ± s.d. Normo = normovascular.
*†‡$p < 0.05$.

DISCUSSION

Regional accumulation of ^{201}Tl, which biologically behaves like potassium, is related to the changes in blood-brain barrier (BBB) permeability, regional blood flow and increased pumping of this potassium analog directly into malignant tumor cells by the (Na+-K+)-ATPase pump (*4,7*). Brismar et al. (*15*) reported that the cellular uptake mechanism for ^{201}Tl was passive in glioma cell lines according to Nernst's equation and not (Na+K(Tl))-ATPase-dependent transport. This distinction is important in conditions in which the membrane potential can be decreased due to elevated extracellular [K+] which causes reduced uptake, although the Na+/K+ pump is functioning and the cells are viable (*16,17*). Also, ^{201}Tl uptake is related to cell growth rates (*16*). In fact, our data suggest that as thallium uptake increases, tumor cell proliferation observed by the PCNA but not the Ki-67 index was higher.

Given the effectiveness of ^{201}Tl imaging in patients with brain tumors, it might be expected to play a substantial role in the prognosis of these patients. Clinical assessment of the response to therapy is a major problem in the follow-up of patients with high-grade astrocytoma. Deterioration of clinical symptoms in a patient with a high-grade astrocytoma may be caused either by radiation therapy or to tumor recurrence. CT and MRI, however, are often unable to make this distinction. Thallium-201 imaging may play a role, in evaluating tumor grade and assessing the affect of therapy.

Visual Analysis in Brain Tumors

Our data suggest that ^{201}Tl accumulated in both astrocytic tumor and benign brain tumors. Several researchers have focused on the relationship between ^{201}Tl uptake and

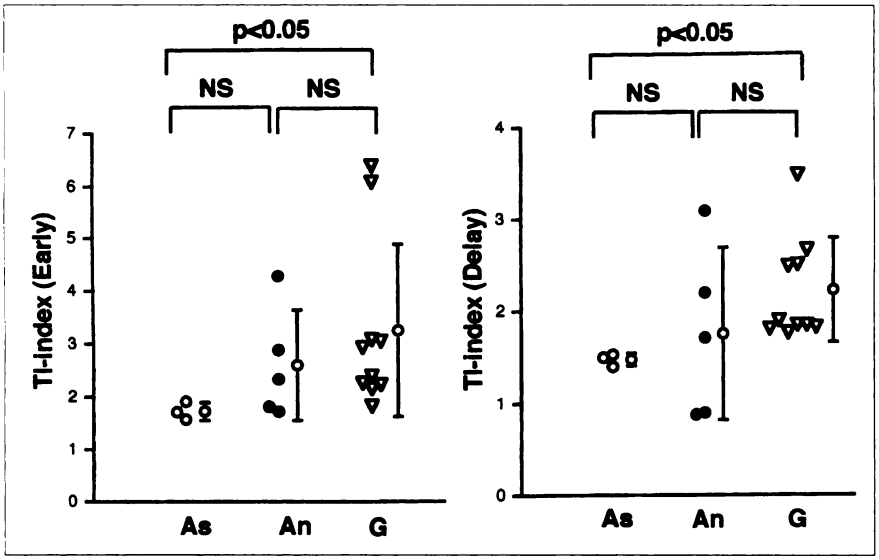

FIGURE 1. Relationship between ^{201}Tl index (early and delay) and astrocytoma (As), anaplastic astrocytoma (An) and glioblastoma (G).

astrocytic tumors. In astrocytic tumors in our study, the lower the grade the lower the ^{201}Tl uptake. Figure 5 showed that there was no significant difference between the ^{201}Tl index in hypervascular and in normovascular or hypovascular tumors on early images. For benign tumors, early ^{201}Tl imaging suggests flow dependency. Furthermore, in astrocytic tumors, there was a large variation for the accumulation grade. There was a tendency for intense uptake in glioblastomas. During image acquisition, we obtained early and 4-hr delayed images. Kim et al. (*8*) obtained ^{201}Tl SPECT images 5 min postinjection. As our data suggest, imaging at 5 min may be strongly influenced by flow (Figs. 4, 5). Therefore, we recommend delayed images for interpreting ^{201}Tl brain tumor images.

Thallium Index in Brain Tumors

Initially, Mountz et al. (*18*) proposed the ^{201}Tl planar image uptake index (^{201}Tl index) of brain tumor counts normalized to cardiac activity. Kaplan et al. (*7*) described that ^{201}Tl uptake was better correlated with residual high-grade glioma tissues than uptake on images with other radiopharmaceuticals such as ^{99m}Tc-glucoheptonate or ^{67}Ga images. Kim et al. (*8*) described strong statistical differences between the ^{201}Tl index in low-grade compared to high-grade brain tumors. In 14 patients with biopsy or autopsy documented low-grade astrocytoma, the mean ^{201}Tl index was 1.27 ± 0.4 compared with high-grade astrocytomas. Using a threshold index of 1.5 to distinguish low- versus high-grade lesions, Kim et al. (*8*) could predict malignancy grade with an accuracy of 89%. Mountz et al. (*19*) noted that the ability of ^{201}Tl to selectively image high-grade astrocytoma was due to its preferential uptake in tumor cells using microautoradiography. These investigators concluded that ^{201}Tl was a useful radiopharmaceutical for preoperative evaluation of brain tumors.

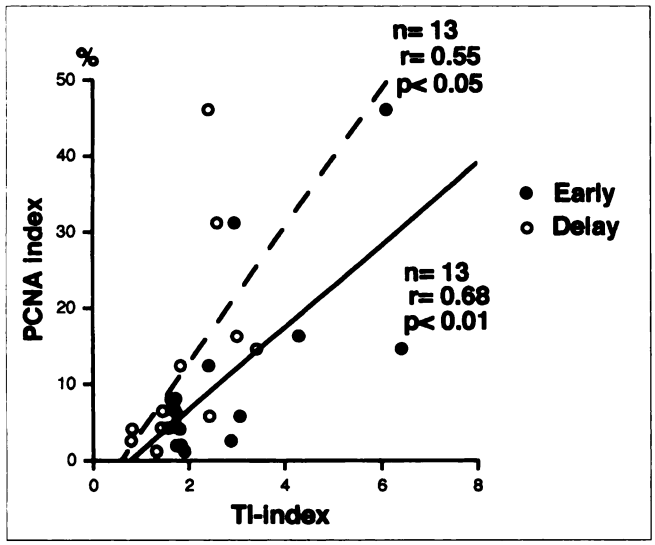

FIGURE 2. Correlation between ^{201}Tl (early/delay) and PCNA indices.

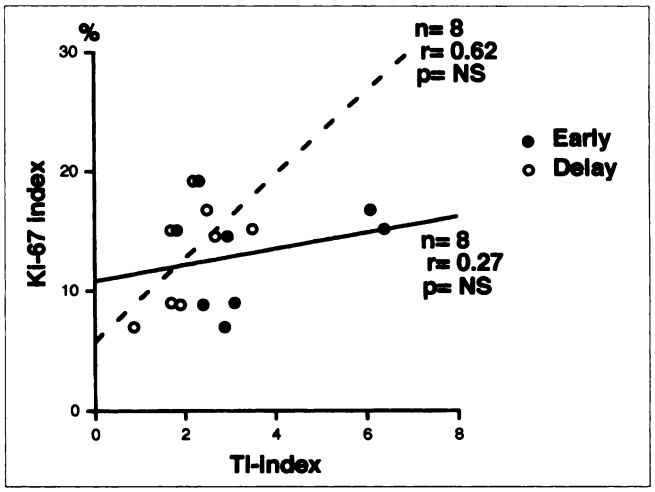

FIGURE 3. Correlation between ^{201}Tl (early/delay) and Ki-67 indices.

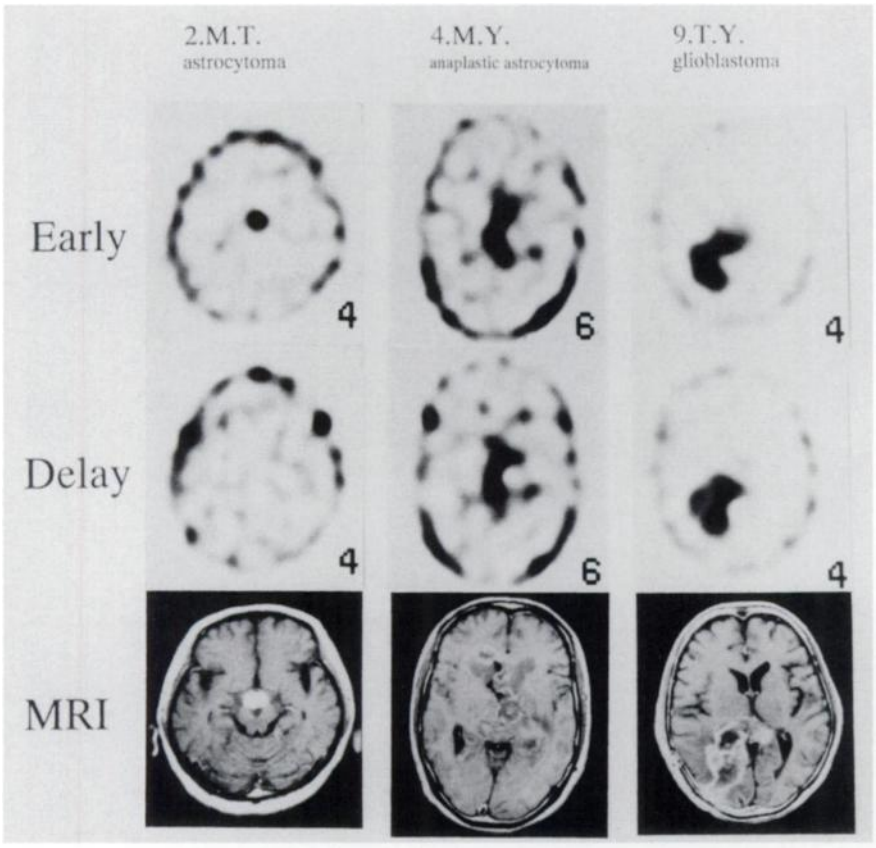

FIGURE 4. Typical ^{201}Tl SPECT images. From left to right: astrocytoma (Patient 2), anaplastic astrocytoma (Patient 4) and glioblastoma (Patient 9) are demonstrated. (Top) Thallium-201 early images, (middle) ^{201}Tl delayed images and (bottom) Gd-enhanced MR images.

Washout Rate

Okada et al. (*20*) examined ^{201}Tl kinetics in the myocardium after intravenous and intracoronary injections using implantable miniature cadmium-telluride radiation detection devices. They described that the factor altering the rate of ^{201}Tl clearance from the blood may also affect the tracer clearance rates from the myocardium. In brain tumors, the factors determining washout were not clear. There was no

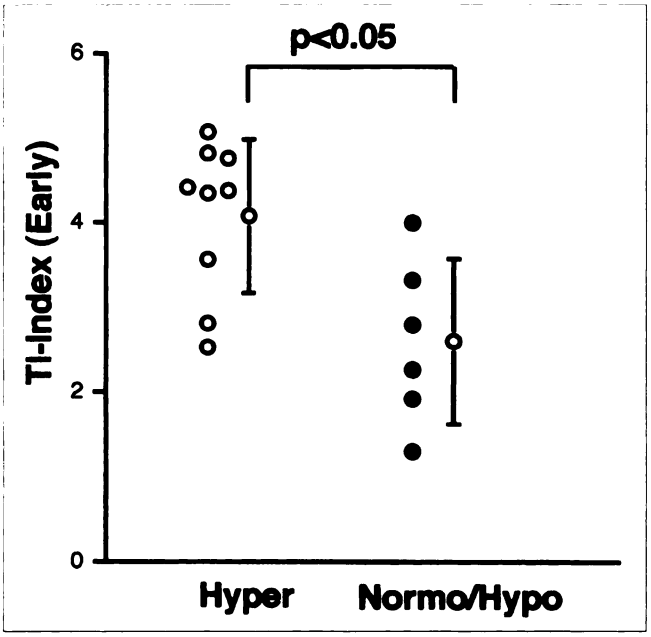

FIGURE 5. Relationship of ^{201}Tl index (early) between hypervascular and normovascular or hypovascular tumors in patients with benign brain tumors.

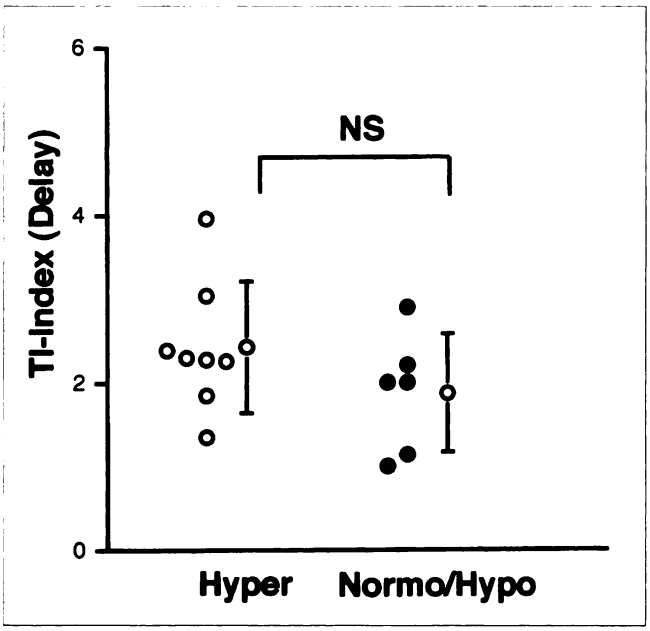

FIGURE 6. Relationship of ^{201}Tl index (delay) between hypervascular and normovascular or hypovascular tumors in patients with benign brain tumors.

significant difference between the Ki-67 or PCNA indices and washout rates in astrocytic tumors.

PCNA and Ki-67 in Brain Tumors

The present study compared PCNA, Ki-67 and ^{201}Tl indices in patients with astrocytic tumor. Recent advances in immunobiology and molecular pathology have led to the development of techniques that can potentially obtain inaccessible information from tumor tissue. Immunocytochemical investigation, using flow cytometry, also revealed that the antigen recognized by the Ki-67 antibody was closely associated with DNA but was not directly associated with either the nuclear matrix or histones (*21*). Also, PCNA functions as a co-factor for DNA synthesis (*22*). In our study, the ^{201}Tl index in the patients with astrocytic tumors was compared to tumor specimens using PCNA and Ki-67.

There was no significant difference between anaplastic astrocytoma and glioblastoma. We could not assess astrocytomas because the study was limited to three patients with this tumor. Also, in brain tumor tissue, it is difficult to mount tumor sections on slides and use Ki-67 due to decreased antigen activity. On the other hand, PCNA is not decreased by its activity. In astrocytoma, there was relatively homogeneous distribution of Ki-67 stained cells, with no areas of frank necrosis. Therefore, counting and averaging a number of fields will provide an accurate measure of the labeling index. Okada et al. (*23*) described a close correlation between Ki-67 positivity and histological grading in malignant lymphoma using FDG-PET. Our data, however, addressed a positive correlation between brain tumor cell proliferation and the ^{201}Tl index. Conversely, FDG-PET is limited by high cost and huge preparation. Thallium-201, on the other hand, is easily available in any hospital. Moreover, Oriuchi et al. (*24*) described the relationship to histologic grade and proliferative activities in the supuratentorial glioma using ^{201}Tl SPECT.

Our data emphasize that the increase in PCNA or the Ki-67 index corresponded to the increase of the ^{201}Tl index. Indeed, the two patients, who had higher ^{201}Tl indices had poor prognoses. Based upon these results, the ^{201}Tl index may be useful in the follow-up of patients with astrocytic tumors. For determining cell cycle times in tumors, further studies could be carried out in astrocytic tumor patients. Furthermore, in benign tumors, the ^{201}Tl index may offer important information on the vascular-rich component in tumor. This may suggest that special attention be paid to the hypervascular element on early images of astrocytic tumors.

CONCLUSION

Overall, the present data show a positive correlation between ^{201}Tl findings and PCNA or Ki-67 monoclonal antibodies, with ^{201}Tl being more accurate in predicting the degree of tumor malignancy. Despite these caveats, it is our contention that ^{201}Tl brain SPECT is an important addition to the armamentarium of noninvasive techniques available for quantitative description of brain tumors.

ACKNOWLEDGMENTS

The authors are grateful to H. William Strauss, MD, Stanford University Medical Center, Stanford, CA and Yoshiharu Yonekura, MD, Kyoto University, Kyoto, Japan for their valuable suggestions and contributions to this study. The authors thank Nihon Medi-Physics Co., Ltd. (Nishinomiya, Japan) for providing the ^{201}Tl.

REFERENCES

1. Hiesiger E, Fowler JS, Wolf AP, et al. Serial PET studies of human cerebral malignancy with [1-C-11]putrescine and [1-C-11] 2-deoxy-D-glucose. *J Nucl Med* 1987;28:1251–1261.
2. Tonami N, Hisada K. Clinical experience of tumor imaging with ^{201}Tl-chloride. *Clin Nucl Med* 1977;2:75–81.
3. Black KL, Hawkins AH, Kim KT, Becker DP, Lerner C, Marciano D. Use of thallium-201 SPECT to quantitate malignancy grade of gliomas. *J Neurosurg* 1989;71:342–346.
4. Ancri D, Basset JY, Lonchampt MF, Lonchampt MF, Etavard C. Diagnosis of cerebral lesion by thallium-201. *Radiology* 1978;128:417–422.
5. Jinnouchi S, Hoshi H, Ohnishi T, et al. Thallium-201 SPECT for predicting histological types of meningiomas. *J Nucl Med* 1993;34:2091–2094.
6. Ancri D, Basset JY. Diagnosis of cerebral metastases by thallium-201. *Br J Radiol* 1980;53:443–453.
7. Kaplan WD, Takvorian T, Morris JH, Rumbaugh CL, Connolly BT, Atkins HL. Thallium-201 brain imaging: a comparative study with pathological correlation. *J Nucl Med* 1987;28:47–52.
8. Kim KT, Black KL, Marciano D, et al. Thallium-201 SPECT imaging of brain tumors: methods and results. *J Nucl Med* 1990;31:965–969.
9. Hoshino T. A commentary on the biology and growth kinetics of low-grade and high-grade gliomas. *J Neurosurg* 1984;61:895–900.
10. Hoshino T, Nagashima T, Murovic JA, et al. In situ cell kinetics studies on human neuroectodermal tumors with bromodeoxyuridine labeling. *J Neurosurg* 1986;64:453–459.
11. Nagashima T, DcArmond SJ, Mouovic J, Hoshino T. Immunocytochemical demonstration of S-phase cells by anti-bromodeoxyuridine monoclonal antibody in human brain tumor tissues. *Acta Neuropathol* 1985;67:155–159.
12. Khoshyomn S, Maier H, Morimura T, Kitz K, Budka H. Immunostaining for proliferating cell nuclear antigen: its role in determination of proliferation in routinely processed human brain tumor specimens. *Acta Neuropathol* 1993; 86:582–589.
13. Louis DN, Edgerton S, Thor AD, Hedley-Whyte ET. Proliferating cell nuclear antigen and Ki-67 immunohistochemistry in brain tumors: a comparative study. *Acta Neuropathol* 1991;81:675–679.
14. Zuber P, Haman M, Tribolet N, et al. Identification of proliferating cells in human glioma using the monoclonal antibody Ki-67. *Neurosurgery* 1988;22: 364–368.
15. Brismar T, Collins VP, Kesselberg M. Thallium-201 uptake relates to membrane potential and potassium permeability in human glioma cells. *Brain Res* 1989;500:30–36.
16. Kimeberg HK, Bowman C, Biddlecome S, Bourke RS. Cation transport and membrane potential properties of primary astroglial cultures from neonatal rat brain. *Brain Res* 1979;177:533–550.
17. Elligsen JD, Thompson JE, Frey HE, Kruuv J. Correlation of (Na+-K+) ATPase activity with growth of normal and transformed cells. *Exp Cell Res* 1974;87:233–240.
18. Mountz JM, Staffoerd-Schuck K, McKeever PE, Taren J, Beierwaltes H. Thallium-201 tumor/cardiac of residual astrocytoma. *J Neurosurg* 1988;68:705–709.
19. Mountz JM, Raymond PA, McKeever PE, et al. Specific localization of thallium-201 in human high-grade astrocytoma by microautoradiography. *Cancer Res* 1989;49:4053–4056.
20. Okada RD, Jacobs ML, Dagget WM, et al. Thallium-201 kinetics in nonischemic canine myocardium. *Circulation* 1982;65:70.
21. Sasaki K, Matsumura K, Murakami T, et al. Intranuclear localization of the Ki-67 reactive antigen in HeLa cells. *Bio Cell* 1990;68:129–132.
22. Carey FA, Fabbroni G, Lamb D. Expression of proliferating cell nuclear antigen in lung cancer: a systematic study and correlation with DNA ploidy. *Histopathology* 1992;20:499–503.
23. Okada J, Yoshikawa K, Itami M, et al. Positron emission tomography using fluorine-18-fluorodeoxyglcose in malignant lymphoma: a comparison with proliferative activity. *J Nucl Med* 1992;33:325–329.
24. Oriuchi N, Tamura M, Shibazaki T, et al. Clinical evaluation of thallium-201 SPECT in supuratentorial glioma: relationship to histologic grade, prognosis and proliferative activities. *J Nucl Med* 1993;34:2085–2089.